

Turbulence Measurements in a Two-Dimensional Upwash

Barry L. Gilbert*

Grumman Corporate Research Center, Bethpage, New York

Early results of an experimental investigation of the abnormally high mixing layer growth rate characteristics found in the upwash regions of V/STOL flows in ground effect are presented. The overall objectives of this program are to characterize systematically the development and structure of the upwash and to determine the parameters that influence these characteristics. The approach adopted is to investigate the fundamental turbulent V/STOL upwash mechanisms in a simplified configuration. In the effort reported herein, a two-dimensional upwash was formed by the collision of opposed two-dimensional wall jets. Extensive measurements were made in the two-dimensional wall jet to establish the starting conditions of the upwash. Evaluation of these measurements shows classical wall jet behavior; and, by the time the wall jet reaches the collision zone, both the mean and turbulence profiles are fully developed. A unique set of velocity profiles obtained at six locations in the upwash is presented. The data include simultaneous X-probe measurements of two components of the velocity in the upwash. The results indicate that the turbulence levels and mixing layer growth rates are larger than those found in a free two-dimensional jet; however, these values are smaller than those previously reported.

Introduction

THE development of aircraft with vertical/short takeoff and landing (V/STOL) capability has led to a requirement for understanding the unique turbulence phenomena encountered in the interaction of lift jets with the ground. When a V/STOL aircraft is in ground effect, the exhaust from the aircraft lift jets interacts with the ground, producing an upwash flow directed toward the underside of the aircraft. The upwash flow has profound aerodynamic implications on the aircraft design. The induced aerodynamic effects due to the upwash augmentation of the lift forces and suckdown entrainment over the lower surfaces of only 5% of the engine thrust may translate into as much as a 40% difference in mission payload or endurance. An understanding of the basic physical mechanisms acting in the flowfield between the aircraft and the ground is vital to the successful development of a practical V/STOL aircraft. The upwash flow behavior is very difficult to analyze due to a much greater mixing layer (fan width) growth rate compared to other types of turbulent flows.^{1,2}

Although a number of investigations of overall flow in ground effect have been carried out, measurements in these highly unsteady flows are very difficult and interpretations of these measurements vary widely.³⁻⁸ The problem is made computationally difficult by the intrinsic three-dimensionality of the upwash. However, even when these difficulties are overcome, the numerical codes require better definition of the turbulent structure in order to make reliable predictions of the fountain flow and, later, the fountain/aircraft interaction. Aircraft designers currently use models derived from relatively crude approximations and semiempirical correlations and/or very expensive large-scale wind-tunnel tests that preclude by their cost-sufficient data to understand the flow adequately.

Previous investigations have attempted to study the full V/STOL flowfield with its full geometric complexity. Some of these have even made measurements with an aircraft planform. These are configuration specific studies that necessarily

miss the fundamental flow characteristics. Our approach was to employ a simple two-dimensional flow configuration. In this configuration, the complex V/STOL upwash flow geometry is simplified. The lifting jet impingement region with the ground is eliminated and the radially spreading wall jets are replaced by the much simpler two-dimensional wall jets. This study has the goal of producing a baseline data set showing the increased mixing rate.

This paper includes details of the design and construction of the experimental apparatus used to produce the two-dimensional upwash, sufficient measurements to assure two-dimensionality and uniformity of the exit profiles, and detailed measurements of the wall jet profiles to assure that the wall jets were well behaved. These measurements are very important, since these two-dimensional wall jets represent the initial flow conditions into the formation region of the upwash. An X-probe hot-film anemometer was used to measure mean and turbulence profiles at six locations in the upwash. These measurements form a comparison set of data to the relatively small sample of upwash measurements that exists in the current literature.

Results

Apparatus

The wind-tunnel facility designed and constructed for this study is diagrammed in Fig. 1 and the test section is shown in Fig. 2. Each of two independent fans drives the flow through identical, 90 cm long, 26.5 deg half-angle, subdivided diffusers. The plenum chamber has a honeycomb, three sets of 16 mesh/in. screens, and a gentle balsa contraction. The nozzle section employs a symmetric ASME long-nozzle contraction to a 10 cm height followed by an asymmetric lemniscate curve contraction to an exit height D_w of 1 cm. The nozzle geometry was carefully chosen to minimize the interference to the entrainment flow over the top of the nozzle. The success of this design can be seen later in the nozzle exit profiles. The exit aspect ratio is 50:1. The test section has plexiglass side walls to aid in maintaining the two-dimensionality of the flow. The ground plane is instrumented with static pressure taps connected to pressure transducers capable of high-frequency response. To facilitate comparisons with conventional data, a coordinate system is used that allows the X direction to be in the direction of the largest velocity component. That is, X tracks some centerline streamline and Y is always perpen-

Presented as Paper 83-1678 at the AIAA 16th Fluid and Plasma Dynamics Conference, Danvers, MA, July 12-14, 1983; received Sept. 2, 1986; revision received May 11, 1987. Copyright © 1987 by B.L. Gilbert. Published by the American Institute of Aeronautics and Astronautics, Inc., with permission.

*Senior Research Scientist, Aerosciences. Senior Member AIAA.

pendicular to it. This results in a 90 deg rotation of X from the wall jet to the upwash as shown in Fig. 3. Therefore, for clarity, wall jet parameters are subscripted with w . U and u' , V and v' are the mean and fluctuation components in the X and Y directions, respectively.

The facility has the capability of producing two independently controlled wall jets with flow rates that may be set equal up to an exit velocity of 67 m/s. Figure 4 shows hot-film anemometry measurements of a typical exit plane velocity profile taken vertically across the nozzle exit and includes the entrained flow velocity over the top of the nozzle. There is negligible variation in the exit profiles taken at various locations across both nozzles. The flow is uniform to 0.5% across the 50 cm long dimension excluding the regions near the ends of the nozzle. Disregarding the boundary layer, the mean velocity is uniform to 0.75% with turbulent intensities u'/U of about 0.6%. The single-jet external entrainment velocity increases from about 6.6% of the mean exit velocity to 9.7% when both wall jets are used to form an upwash. The instrumentation plate is 84 cm long (nozzle to nozzle).

Wall Jet Measurements

It is possible to get a good qualitative estimate of the size of the collision zone. A single mean velocity trace was made at a height of $Y_w/D_w = 0.5$ from the exit to a point past the centerline collision zone. With only one jet on, the first trace shown in Fig. 5 shows the expected linear decay required by the conservation of momentum. The second curve shows the mean velocity at the same height above the ground using both jets. In the interference zone, interpretation of velocity direction is not possible from single-probe measurements. The single-wire constant temperature anemometer, with the sensor perpendicular to the page, measures the velocity component normal to its axis, that is, the component in the plane of the page composed of the vector sum of $U + V$. Two features of these curves are important: 1) the effect of the second jet is confined to the collision zone as shown by the unaffected decay tract from the jet exit to the zone and 2) as will be shown in the next set of plots, the wall jet layer would be of the order of four nozzle heights at the centerline if the second jet were not running. One would expect the collision zone to be twice this wide (consistent with Ref. 3). Figure 5 shows the collision zone to be of that order.

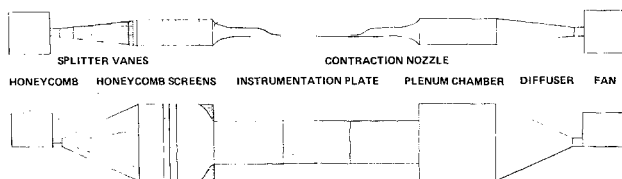


Fig. 1 Diagram of two-dimensional jet upwash facility.

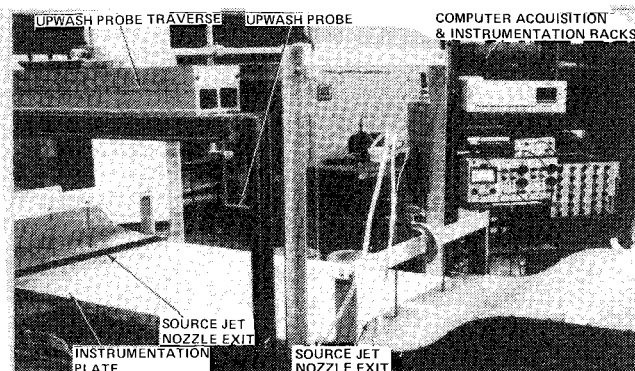


Fig. 2 Two-dimensional jet upwash facility.

Wall jet mean and turbulence profiles were taken at 20 locations from the jet exit nozzle to the instrumentation plate centerline. These profiles were made at equal distances along the plate in increments of approximately two nozzle heights. Each profile contains 24 data points. The measured variation in probe position above the plate from the first to the last profile position was less than 0.13 mm. The data acquisition and positioning of the single element hot-film probe were accomplished under the total control of the automatic digital data system.

A plot of the wall jet growth rate as characterized by the half-velocity height vs the distance downstream is given in Fig. 6a. The half-velocity height is the usual length scale used to characterize wall jets. It is the height (above the maximum velocity point) where the mean velocity is half the maximum velocity. A linear least-squares curve fit of the data from stations 6–20 ($40 > X_w/D_w > 10$) gives a growth rate of 0.0728. This is exactly the growth rate established as the “correct” value for self-preserved two-dimensional wall jets on plane surfaces at the 1980–81 AFOSR-HTTM Stanford Conference⁹ of 0.073 ± 0.002 . The first five stations were eliminated from the curve fit because they appeared to be in the development

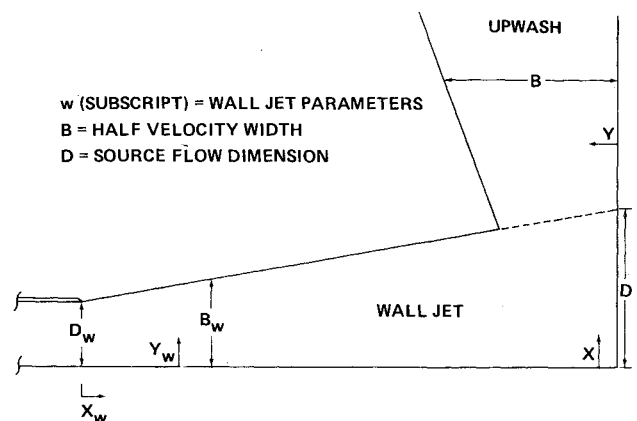


Fig. 3 Coordinate system nomenclature conversion.

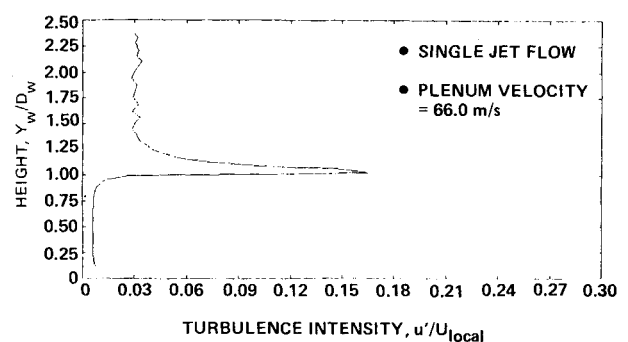
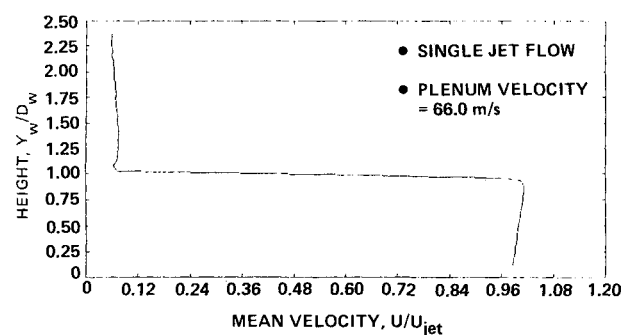


Fig. 4 Typical jet exit velocity profiles.

region. Figure 6b shows the linear decay of the maximum velocity squared vs distance. This relationship is required by conservation of momentum considerations. The mean velocity similarity exists as early as $X_w/D_w = 10$, much sooner than the 50 slot heights quoted at Stanford. The turbulence profiles normalized by the half-velocity width show similarity at X_w/D_w about 20. The wall jet characteristics at the centerline of the collision zone may be determined. From Fig. 5, it was noted that the collision process is a very local phenomenon. When no collision occurs, the wall jet parameters should be used to normalize the upwash data in a manner similar to using the wall jet nozzle height as an initial characteristic dimension and the source jet velocity as the characteristic velocity. At the centerline, the wall jet half-height is $B_w/D_w = 3.702 = D$ for the upwash and $U_{\max}/U_{\text{jet}} = 0.571 = U_0$.

Upwash Measurements

The upwash profiles were measured using an X-probe hot-film anemometer. This measurement technique is able, with proper electronic manipulation, to sense two perpendicular instantaneous velocity components. Using this technique, two component mean velocity profiles at the same six heights of $1.35\text{--}8.11D$ in $1.35D$ increments were obtained by an automatic data acquisition process. These were mean velocity profiles in the direction of the upwash X and also the mean component into the upwash Y as entrainment or as spreading. These data were obtained by digitizing 4000 data pairs in 1.5 s from each wire of the X-probe. The digital technique gives value of component turbulence energy that are 98% of the values measured by a simultaneous analog technique. In addition to the mean (average) value from the new time series, the turbulent intensity (deviation) in each direction and one component of the Reynolds stress (cross product) were also obtained.

The mean velocity components in the upwash direction are shown in Fig. 7. At the first height, $X/D = 1.35$, the data do not follow the trend of the data at the other five locations. This trend will be very obvious in successive plots. These data are shown plotted in similarity form using normalizing parameters determined by the curve fit described later. There is a great deal of information that can be obtained from these data. The residual velocities in the tails are similar to other studies.³⁻⁸ This flow in the tails is the entrainment flow toward the center, perpendicular to the upwash direction. This has been verified by smoke flow visualization studies. The mean velocity profiles are symmetric; beyond $H/D = 2.70$, the turbulence profiles have symmetric peaks. These turbulent profile data are not given in Ref. 5; Refs. 4 and 6 show only one-sided turbulence measurements, that is, they do not show the symmetric data. Only Refs. 3 and 8 show the complete profiles.

Figure 8 shows the cross-stream mean velocity component normalized by the local maximum velocity. Looking at the data at the higher stations shows the mean spreading velocity to the right on the right-hand side and the symmetric mean spreading velocity (negative values) to the left, left of the center. These profiles are symmetric about the upwash velocity maximum. At the lowest station, $X/D = 1.35$, these trends are reversed. That is, for example, there is an inflow from the right of center. Remember that $X = D$ would be, by definition, the position where the wall jet velocity is half the local wall jet maximum. For X slightly larger than D , the wall jet still has a velocity component toward the centerline, which appears as a cross-upwash direction component. This is a direct indication that $X/D = 1.35$ is still in the interference collision zone. That is, the inflow velocity to the right and left of center is really the wall jet flow.

Figures 9 and 10 show the normalized component turbulent energy in the upwash and relative turbulence energy in the cross-stream direction, respectively. The forms and magnitudes of these profiles are similar to those expected for two-dimensional free jet flows.

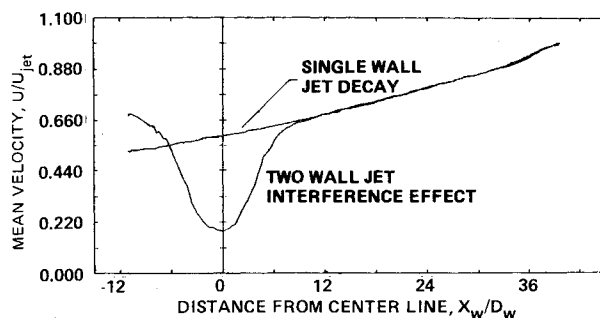
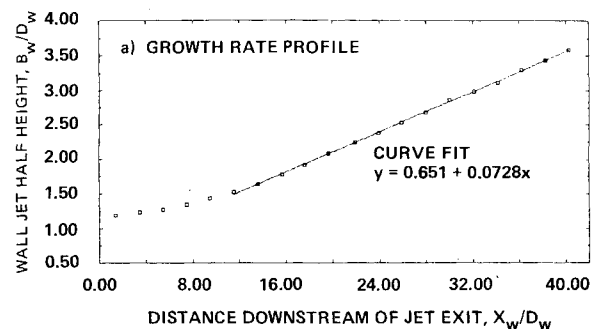
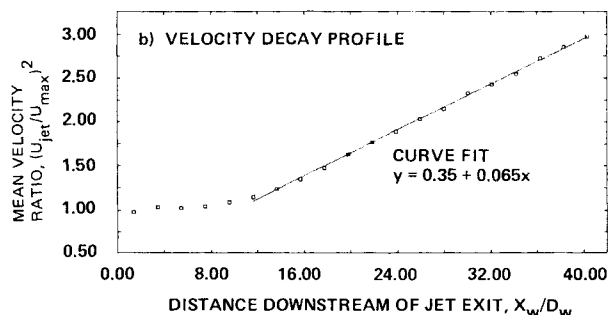


Fig. 5 Mean velocity decay trace at $Y_w/D_w = 0.5$ with a single-wall jet and with colliding wall jets.



a) Growth rate profile.



b) Velocity decay profiles.

Fig. 6 Two-dimensional wall jet characteristics.

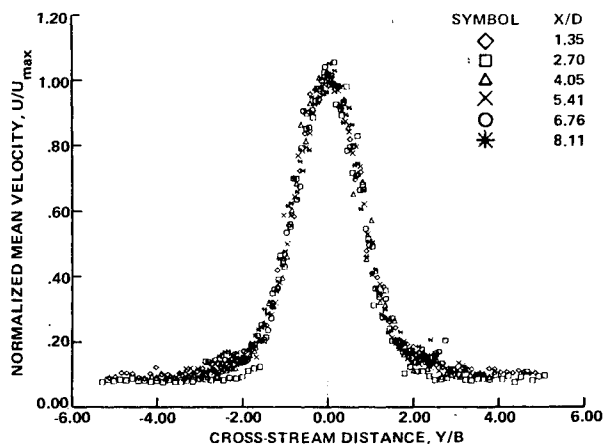


Fig. 7 Mean velocity profiles for two-dimensional upwash at six heights in similarity form.

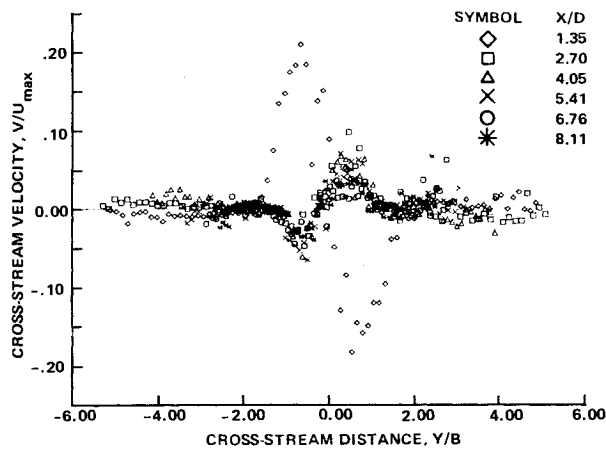


Fig. 8 Cross-stream velocity for two-dimensional upwash at six heights.

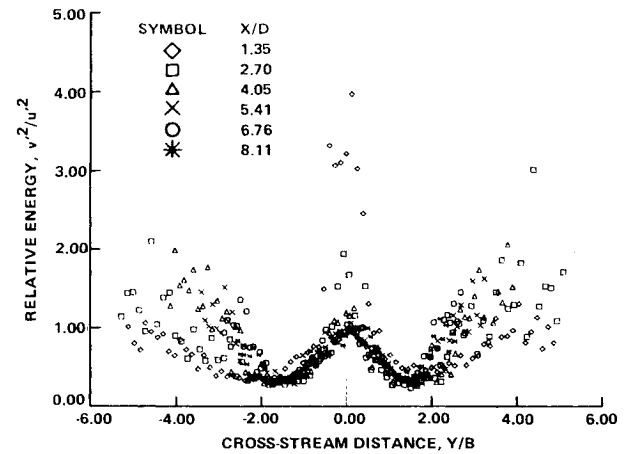


Fig. 10 Relative turbulence energy in two-dimensional upwash at six heights.

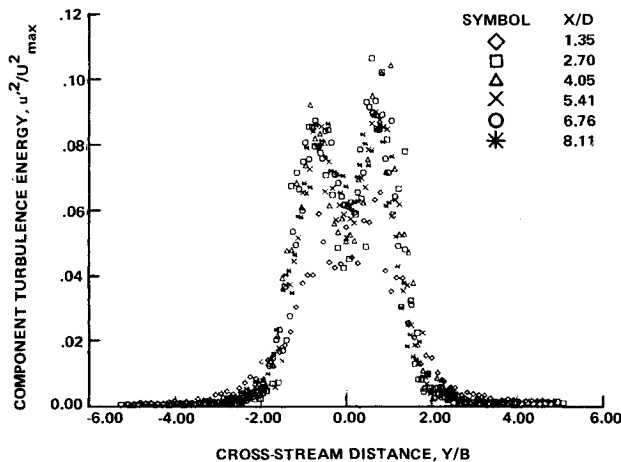


Fig. 9 Component turbulent energy for two-dimensional upwash at six heights.

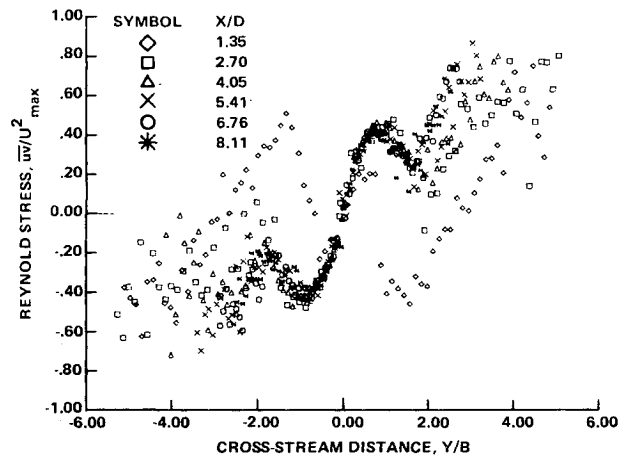


Fig. 11 Reynold stress for two-dimensional upwash at six heights.

Preliminary evaluation of the turbulence levels found in the upwash shows these values to be only slightly higher than those found in ordinary two-dimensional free jet flows. This is contrary to statements made by Foley and Finley⁶ and Witze and Dwyer⁴ that the turbulence intensity is a factor of three greater than the free jet case. However, examination of their published data indicates ordinary levels. Kind and Suthanthiran³ show factors of three. Kotansky and Glaze⁵ show no turbulence data at all. The recent paper by Saripalli⁸ uses a two-component laser Doppler velocimeter to make measurements in the upwash formed by impinging free jets in a water tunnel. While he did find an increased growth rate, it is smaller than reported here. However, that paper reports turbulence levels and shear stresses of tremendous magnitude. He reports values of turbulence energy that are nearly twice the free jet values and stresses nearly four times those values. The decreased growth can be due to the confining effect of the impinging jets. The increased turbulence is due in part to a seeding technique that allows measurements of only the source fluid in the upwash. No explanation is given for these levels. The local values of turbulence intensities measured here (i.e., the rms of the fluctuations normalized by the local mean) are on the order of 60%. This is well in excess of the range of application of the small-perturbation approximation used to evaluate turbulence properties in the thermo-anemometry.

Figure 11 shows one component of the Reynolds stress uv/U_{\max}^2 . Again, looking to the higher stations first, across the center region the Reynolds stress profiles are asymmetric

about the centerline and the same magnitude on either side. Since Reynolds stress measurements are particularly sensitive to measurement techniques, these plots are an indication of the good precision obtained in these experiments. Plotted as a correlation coefficient normalized by the rms values, the scatter in the tails is due to normalizing by successively smaller values. Again, at $X/D = 1.35$, the entire profile is reversed.

The mean velocity profiles in the upwash direction were curve fit with a least-squares curve of the form $U = A + C \exp[-(y - y_0)^2/2S^2]$. This curve fit gives the symmetry coordinate y_0 (shown in Fig. 12), the maximum velocity $(A + C)$, and the standard deviation S . Using the generally accepted definition of the half-velocity width, $B(U = U_{\max}/2) = 1.77 S$. It should be emphasized that this technique is far superior to the usual determination of the half-width. That procedure usually entails finding U_{\max} and interpolating between data points to determine B . The method suffers severely from scatter in the data at both U_{\max} , particularly at the half-velocity point. Also, it rarely gives symmetric half-velocity positions. A least-squares curve fit avoids these problems.

The results of the half-velocity growth rate so derived are shown in Fig. 12a. The upwash growth rate is about 0.21 compared to values of about 0.37 reported by Witze and Dwyer,⁴ for example. However, this value is still more than twice the value found in free jets. A closer look at these other data shows inconsistency and, in some cases, plotted data disagree with written statements. We believe our data are correct. The proper mean velocity decay characteristic is shown for X/D

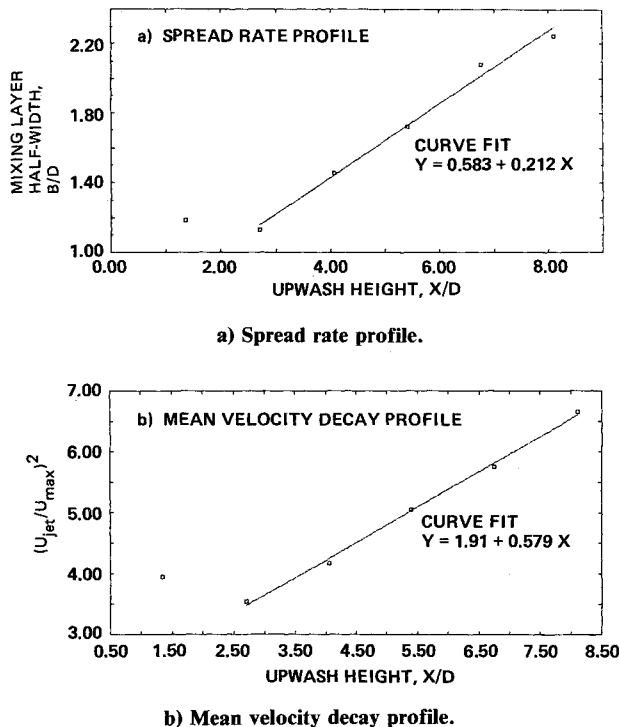


Fig. 12 Two-dimensional upwash characteristics.

greater than 2.70. This is the form for the mean velocity decay required by conservation of axial momentum in the upwash, a characteristic not usually found by others. Between $X/D = 1.35$ and 2.70, the mean velocity actually increases and the mixing width decreases correspondingly. This is a strong indication that the extent of the collision zone is between $1.35D$ and $2.70D$, consistent with decay trace shown in Fig. 5. The $X/D = 1.35$ data were again not used in the curve fit because, at this height, the profile is not fully developed. Finally, Fig. 12b shows the mean velocity decay relationship required by conservation considerations.

Using these relationships, the similarity form of the mean velocity profile is given by the expected expression $U/U_{\max} = \exp[-0.693 (Y/B)^2]$. The constants in the curve fits have been absorbed into virtual origin shifts. However, because the mixing layer growth rate is twice the free jet value, the similarity profile can be given as $U/U_{\max} = \exp[-15.5 (Y/X)^2]$, where the free jet coefficient is between 70.7 and 75.0. Since the mixing layer growth rate is higher, the mean velocity decay must be correspondingly lower. Our decay curve is $U_{\max}/U_0 = 0.750/\sqrt{(X/B)}$ compared to a coefficient of about 3.50 in the free jet case.

The entrainment coefficient can now be estimated from the mean velocity decay and growth rate relations used in the conservation equations. By assuming that the entrainment velocity is a constant fraction of the local maximum velocity, the fraction is given as 0.53 times the growth rate. In the free jet case for a growth rate of 0.1, this is about 0.053. Here, the entrainment velocity is significantly higher at 0.112 of the local maximum velocity. This is readily seen in smoke-flow visualization studies. The entrainment velocity represents only the magnitude of the velocity-carrying mass into the upwash and is not expected to appear as the transverse velocity component in Fig. 8.

Summary

The data reported in this paper represent the initial results of a fundamental investigation of the turbulence structure found in a V/STOL upwash. The approach was to simplify the flow geometry to a two-dimensional upwash formed by the collision of opposed two-dimensional wall jets. The experimental apparatus is sufficiently generic to provide the scientific computational fluid dynamics community with an important data set for comparison. A basic set of calibration exit profile data has been taken. Wall jet profiles were obtained at 20 locations from the jet exit to the facility centerline. These surveys showed the rapid development of the mean and turbulence similarity profiles. They also exhibited the well-established mixing layer growth rate and mean velocity decay rate that characterize the wall jets. Careful measurements were made at six heights in the upwash using an X-probe hot-film probe. The expected abnormally high mixing layer growth rate was found in the two-dimensional upwash flow. However, the turbulent intensity was of the same order as is found in ordinary two-dimensional free jets. There is basic agreement between our data and prior studies. Although there is some disagreement in specific details (such as the spread rate), our values are within the range found by others. Our set of carefully generated data from a well-defined two-dimensional source shows symmetry of the turbulence energy profiles in the upwash. This baseline upwash data set shows mean velocity decay and spread rate trends required by conservation considerations. Data interpretation was difficult due to directional ambiguity of the hot-film sensor and the high local turbulence levels. These X-probe measurements have shown the cross component mean velocity in the upwash. In addition, the turbulence profiles for both components were obtained. Finally, one component of the Reynolds stress was measured. As a sign of the accuracy of the measurement technique, these cross-component data show remarkable symmetry.

Acknowledgment

This research was funded by the U.S. Air Force Office of Scientific Research under Contract F49620-82-C-0025.

References

- ¹Rajaratnam, N., *Turbulent Jets, Developments in Water Science*, Vol. 5, Elsevier Scientific Publishing, Amsterdam, 1976.
- ²Harsha, P.T., "Free Turbulent Mixing: A Critical Evaluating Theory and Experiment," AEDC-TR-71-36, Feb. 1971.
- ³Kind, R.J. and Suthanthiran, K., "The Interaction of Two Opposing Plane Turbulent Wall Jets," AIAA Paper 72-211, Jan. 1972.
- ⁴Witze, P.O. and Dwyer, H.A., "Impinging Axisymmetric Turbulent Flows: The Wall Jet, the Radial Jet and Opposing Free Jets," *Proceedings of Symposium on Turbulent Shearflows*, Vol. 1, University of Pennsylvania Press, University Park, April 1977.
- ⁵Kotansky, D.R. and Glaze, L.W., "The Effects of Ground Wall-Jet Characteristics on Fountain Upwash Flow Formation and Development," AIAA Paper 81-1294, June 1981.
- ⁶Foley, W.H. and Finley, D.B., "Fountain Jet Turbulence," AIAA Paper 81-1293, June 1981.
- ⁷Jenkins, R.A. and Hill, W.G. Jr., "Investigation of VTOL Upwash Flows Formed by Two Impinging Jets," Grumman Corp., Bethpage, NY, Research Dept. Rept. RE-548, Nov. 1977.
- ⁸Saripalli, K.R., "Laser Doppler Velocimeter Measurements in 3-D Impinging Twin-Jet Fountain Flows," AIAA Paper 85-4036, Oct. 1985.
- ⁹Kline, S.J. et al. (eds.), *Proceedings of the 1980-81 AFOSR-HTTM-Stanford Conference on Complex Turbulent Flows*, Stanford University Press, Stanford, CA, 1981.